



An easy way to predict and direct the porous structure of activated carbons derived from petroleum asphalt

Oxana V. Gorbunova¹ · Olga N. Baklanova¹ · Tatiana I. Gulyaeva¹ · Anastasia V. Vasilevich¹ · Alexey B. Arbuzov¹ · Mikhail V. Trenikhin¹ · Alexander V. Lavrenov¹

Received: 10 May 2023 / Revised: 25 March 2024 / Accepted: 26 March 2024 / Published online: 7 April 2024
© The Author(s), under exclusive licence to Springer Science+Business Media, LLC, part of Springer Nature 2024

Abstract

The carbonization temperature of carbon precursors before their activation is an important factor affecting the porous structure and properties of the resulting activated carbons. In this work correlation between the textural and adsorption properties of asphalt-based porous carbons and the carbonization temperature has been found. Additionally, the optimal carbonization temperature, and reasons why the carbonization temperature affects the main textural characteristics of the activated carbon were established. A series of porous carbons has been prepared from petroleum asphalt by a two-stage method, including carbonization of asphalt at different temperatures from 450 to 800 °C and KOH activation. To reveal the reasons of the correlation the carbonized samples were studied by TG-DTG, IR-Fourier, TEM methods. It is shown that the carbonization temperature effects on the structural defects, distance between the graphene layers, the reactivity and thermal stability of the carbonized asphalts. These specificities contribute to formation of porous structures of the activated carbons. The carbonization temperature 500–600 °C of the petroleum asphalt is found to be the optimal for further activation. The KOH activation of the petroleum asphalts carbonized at 500–600 °C provides microporous carbon with the high specific surface area (about 2000 m²g⁻¹) and the CO₂ uptake (3.3 mmolg⁻¹). Additionally, the specific surface area of the activated carbons is shown can be predicted from the temperature of 50% (T_{50%}) mass loss of the carbonized petroleum asphalt. The linear dependence of the T_{50%} on BET surface area can be fitted by $T_{50\%} = 640 - 0.424S_{\text{BET}}$ with determination coefficient R² equal to 0.96.

Keywords Porous carbon · Asphalt · Carbonization temperature · KOH activation · CO₂ adsorption

1 Introduction

Important advantages of carbon materials are stability in chemically aggressive environments, large specific surface area, and the ability to control parameters of their porous structures over a wide range. Commercial activated carbons (ACs) usually contain all kinds of pores. Charcoal and mineral coal are usually characterized by large volumes of micropores (up to 0.2–0.4 cm³g⁻¹) and macropores (up to 0.5–1.0 cm³g⁻¹), whereas the volume of mesopores is usually low. It is possible to achieve even larger micropore volumes

of 0.4–0.6 cm³g⁻¹ by varying the raw materials and technological parameters for the ACs synthesis [1]. Microporous ACs are highly efficient in the sorption processes and separation of gas mixtures. Mesoporous ACs are appropriate for sorption processes in liquid-phase. Macropores are usually the transport channels, and their role in the sorption processes of is insignificant.

ACs can be produced from various raw materials, such as wood [2], coal [3], polymers [4], and nutshells [5]. Heavy refining residues (petroleum coke, bitumen, asphalt) are also actively used to produce ACs due to the low cost and high carbon content [6, 7]. Low cost asphalt is produced in vast quantities, but it does not find a qualified application [8]. Since the carbon content of asphalt is more than 85%, it makes asphalt an excellent raw material to produce carbon materials with high yields. The asphaltene included in the composition of asphalt form nanosized conjugated aromatic structures those form porous asphaltene aggregates [9, 10].

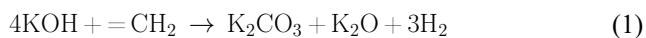
✉ Oxana V. Gorbunova
Oxana_Gorbunova@inbox.ru

¹ Center of New Chemical Technologies BIC, Boreskov Institute of Catalysis, Neftezhavodskaya Str., 54, Omsk 644040, Russian Federation

Activation of asphalts is a well-known way to obtain micro- and mesoporous carbon materials with a large surface area and excellent adsorption properties [11, 12]. For example, Liang et al. [12] prepared AC from petroleum asphalt by varying the KOH/asphalt ratio and activation temperature. It was shown that the obtained carbon material exhibits adsorption properties comparable to the commercial materials.

Industrial technologies for producing activated carbons usually consist of two stages: carbonization and activation of carbon-containing precursors [13]: (i) carbonization is a heat treatment of carbon-containing raw materials in inert atmosphere at temperatures of 600–800 °C with a certain rate of temperature rise, and exposure; (ii) activation is a heat treatment of the carbonized product in an oxidizing atmosphere (H₂O, CO₂, O₂, air) at temperatures of 600–900 °C for 5–120 min, or heat treatment of the carbonized raw material in an inert atmosphere in the presence of activating agents (ZnCl₂, H₃PO₄, KOH, K₂CO₃, NaOH, Na₂CO₃).

Alkali metal hydroxides stand out among the many activating agents. Potassium and sodium hydroxides are one of the most effective activating agents for obtaining microporous carbon materials with high specific surface area and pore volume [13]. KOH is more effective than NaOH. Chemical reactions between hydroxides (KOH or NaOH) and carbonized asphalts occurring in the activation process determine the extension of porosity in ACs. In paper [14], the interaction of alkali metal hydroxides with carbon was studied. The authors had proposed the following mechanism of the activation process:



It can be seen that =CH₂ groups react with KOH to form K₂CO₃ and K₂O. Thus, alkyl groups on the surface of the carbon precursor play a key role in its activation. As a rule, the activation with potassium hydroxide leads to the formation of micropores predominantly. These pores are responsible for the high specific surface area and pore volume [14].

The carbonization temperature is an important factor affecting the properties of the carbon precursor before its activation and, ultimately, the properties of the resulting activated porous carbons [7, 15, 16]. Heating promotes the removal of volatile substances. Therefore, the composition of the carbonaceous raw material after carbonization changes with the carbonization temperature. The size and orientation of crystallites in carbon precursors also depend on the carbonization temperature [17]. Thus, the textural and adsorption properties of the final carbon materials are

determined not only by the activation conditions, but also by the characteristics of the carbon precursor. The properties of the heat-treated carbon precursor also might vary depending on the temperature and duration of carbonization.

In work [18], the duration and temperature of petroleum asphalt pre-carbonization were optimized to obtain ACs with the extended porous structure and high CO₂ capacity. Continuing that study, here we set a primary purpose to establish reasons why the carbonization temperature affects the main textural characteristics of the activated carbon. It was an additional aim of this work to establish the preparation conditions of activated carbons from petroleum asphalt, which can be a promising feedstock for cheaper activated carbons. We have synthesized carbon samples from petroleum asphalt by carbonization at various temperatures followed by activation using KOH. Obtained carbon materials differ in terms of porous structure and ability to adsorb CO₂.

2 Experimental

2.1 Materials

Petroleum asphalt provided by PJSC “Gaspromneft” has density of 1.05 g/cm³. According to ASTM D6560 the asphalt comprises 86.9 wt % of carbon, 9.1 wt % of hydrogen, 2.4 wt % of sulfur, 0.8 wt % of oxygen, 0.7 wt % of nitrogen and 11.5% of asphaltenes. Potassium hydroxide (KOH, purity ≥ 86%) was purchased from Khimprom.

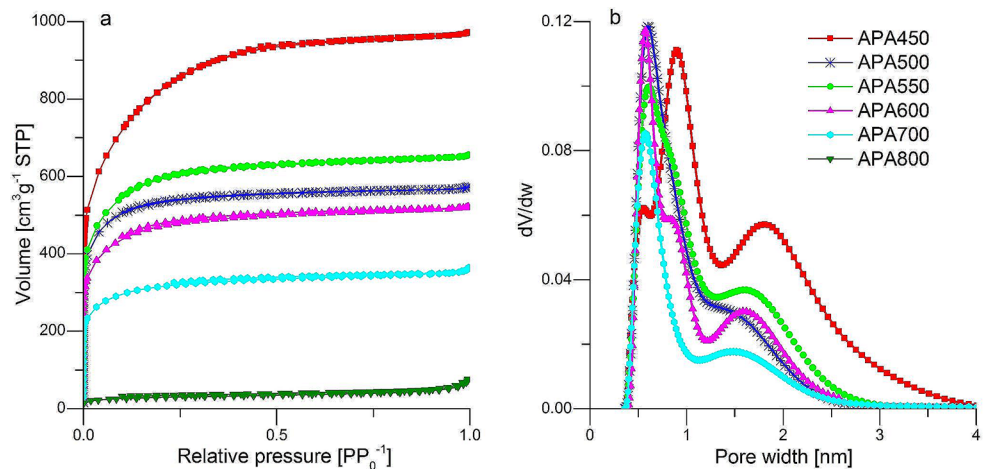
2.2 Carbonization of petroleum asphalt

Asphalt is used as raw material. It was carbonized in argon flow at various temperatures (450 °C, 500 °C, 550 °C, 600 °C, 700 °C and 800 °C) for 1 h. The petroleum asphalt sample carbonized at 450 °C is denoted as PA450. Other samples are marked in the same way. Further, the obtained carbon precursors were activated.

2.3 Preparation of activated carbons

A 1.0 g of carbonized petroleum asphalt was mixed by dry milling with 4 g of KOH as the activating agent at room temperature. The resulting mixtures were put into a horizontal pipe reactor for the activation. The samples were activated as follows: (i) temperature-programmed heating with the ramping rate of 5 °C/min in argon flow from room temperature to 800 °C, (ii) holding at 800 °C for 60 min and then (iii) cooling down to room temperature in argon flow. The activated samples were washed with distilled water until the filtrate appeared neutral. When discussing the results, the

Fig. 1 Nitrogen adsorption isotherms at 77 K on the synthesized activated carbons (a) and differential 2D-NLDFT pore size distributions (b)



activated samples are marked as APAx, where x represents the carbonization temperature.

2.4 Characterization

The nitrogen adsorption-desorption isotherms at 77.4 K were measured for the ACs on the ASAP-2020 M (Micromeritics) analyzer using standard continuous procedures. ACs samples were degassed at 300 °C for 8–10 h under reduced pressure prior to the adsorption-desorption experiments. We have calculated the following texture characteristics: BET specific surface area (S_{BET}), specific pore volume (V_{total} at $P/P_0=0.99$), specific volume of micropores (V_{micro}) by α_s -method. The pore size distribution (PSD) was estimated from the N_2 adsorption isotherms with the non-local density functional theory for heterogeneous surfaces (2D-NLDFT) [19]. 2D-NLDFT model implemented in the SAIEUS software (Micromeritics), free version.

CO_2 adsorption isotherms at pressure up to 1 bar and temperature 25 °C were obtained for the ACs samples on the Sorptomatic 1900 (Carlo Erba Instruments). The samples were degassed at 300 °C for 3 h before the measurements.

Thermal stability of the carbonized petroleum asphalt was measured with the DTG-60 TG/DTA analyzer (Shimadzu) from 30 to 800 °C at the heating rate of 10 °C/min under air atmosphere.

The morphologies and microstructures of the carbonized asphalt samples were characterized by transmission electron microscopy JEM 2100 (JEOL) at accelerating voltage of 200 kV and resolution of 0.14 nm. Computer processing of the electron microscopy images and Fast Fourier transformed (FFT) electron diffraction patterns was made with the Gatan Digital Micrograph software [20].

Surface functional groups of the carbonized carbons were identified using the Fourier transform infrared (FTIR) spectrometer IRPrestige-21 (Shimadzu). The defect level was

Table 1 Textural properties of the asphalt derived porous carbon

| Sample | S_{BET} , m^2g^{-1} | V_{total} , cm^3g^{-1} | V_{micro} , cm^3g^{-1} | V_{meso} , cm^3g^{-1} |
|--------|---|--|--|---|
| APA450 | 2923 | 1.50 | 0.94 | 0.55 |
| APA500 | 1997 | 0.88 | 0.73 | 0.15 |
| APA550 | 2191 | 1.01 | 0.82 | 0.19 |
| APA600 | 1734 | 0.80 | 0.65 | 0.15 |
| APA700 | 1176 | 0.55 | 0.41 | 0.14 |
| APA800 | 100 | 0.10 | 0.03 | 0.07 |

determined by Raman spectroscopy DXR Smart Raman (Thermo Fisher Scientific).

3 Results and discussion

3.1 Characteristics of porous carbons derived from the petroleum asphalt

Figure 1 shows adsorption-desorption isotherms on APAx samples obtained by the activation of the carbonized asphalt. The APA450 sample has the smooth increase of the N_2 adsorption at $P/P_0=0.1-0.5$ (Fig. 1a). It indicates the presence of small mesopores in the porous structure of the sample [21, 22]. The nitrogen adsorption capacity of the activated carbons obtained from the asphalts decreases when the carbonization temperature rises from 500 to 700 °C. The shapes of adsorption-desorption isotherms for the APA500 - APA700 samples are the same and can be classified as the type I isotherm related to microporous solids according to the IUPAC [23]. As it is seen in Fig. 1a, the activation of carbon sample carbonized at 800 °C produces the carbon material with reduced porous structure (APA800).

The BET surface area and pore volume of the activated carbons calculated from the adsorption isotherms are summarized in Table 1.

Table 1 shows that the carbonization of the petroleum asphalt at 450 °C produces the carbon with the extended

textural characteristics. Increase of the carbonization temperature from 500 to 700 °C leads to a decrease in the specific surface area and pore volume of the samples.

The PSD curves of these samples calculated with 2D-NLDFT method are shown on the Fig. 1b. The sample APA800 is not included in this figure because of a negligible amount of N₂ adsorption. The PSD curve for the APA450 sample evaluated relying on the adsorption branch of the isotherm demonstrates the wide distribution between 0.4 and 4 nm with a predominant impact of the supermicro- and mesopores. The supermicropores and small mesopores of the sample carbonized at 450 °C occur in the activation process as evolution of new pores and expansion of existing pores of the carbonized asphalt [24]. Further increase of the asphalt carbonization temperature leads to a decrease of all the textural characteristics and shift of the PSD curves to the micropores region (Fig. 1b). This effect is explained by the formation of relatively stable carbon structures during carbonization at temperatures above 450 °C. If that stable carbon structures occur, the oxidative activation is hampered and the pores do not swell. The ACs samples carbonized at temperatures of 500–600 °C have similar porous structures (Fig. 1a and b; Table 1), with 0.4–2.0 nm micropores.

A good CO₂ adsorbent is known to have a hierarchically porous structure. Macropores and mesopores advantage the mass transport with minimal diffusion resistance, while micropores and especially ultramicropores favor high CO₂ loadings and adsorption selectivity [25]. These facts allow us to suggest the synthesized ACs as good candidates for CO₂ adsorbents. Adsorption capacities of the petroleum asphalt-derived porous carbons for CO₂ have been measured at 25 °C and pressures at 1 bar. Figure 2 shows the CO₂ adsorption isotherms and CO₂ uptake. As can be seen, the ACs samples obtained from the asphalt carbonized in the temperature range of 500–600 °C demonstrate the highest CO₂ uptake. Thus, this carbonization temperature range is optimal for the preparation of microporous carbon

materials having both the high specific surface area (about 2000 m²g⁻¹) and the highest CO₂ uptake (3.3 mmol g⁻¹).

Since the carbonization temperature was shown to have the significant effect on the porous structure of the asphalt-derived carbons, we also have studied the synthesized carbonized samples by TG-DTG, IR-Fourier, TEM methods to reveal the reasons.

3.2 Characteristics of the carbonized petroleum asphalt

Thermal stability of the carbonized petroleum asphalt samples was studied using the thermogravimetry and differential thermal analysis. The combustion of carbon materials is usually characterized by a 50% conversion temperature (T_{50%}). This characteristic temperature is determined from the TG curve (Fig. 3a) [26]. As it can be seen, the T_{50%} rises with increase of the asphalt carbonization temperature from 450 to 800 °C. This indicates an increase in the resistance of carbonized asphalt surface to oxidation. Additionally, the 50% conversion temperature T_{50%} was found to near linearly decrease with the BET surface area of obtained activated carbons (Fig. 3b). Thus, the BET surface area of the carbons after activation can be estimated preliminarily using the thermal analysis data for the carbonized asphalt precursor. The linear dependence of the T_{50%} on BET surface area can be fitted by $T_{50\%} = 640 - 0.424S_{BET}$ with determination coefficient R^2 equal to 0.96.

Structure of the carbon precursors is known to have a considerable effect on the chemical activation process [27]. Therefore, we have analyzed the morphology of carbonized asphalt samples with transmission electron microscopy (TEM). Typical TEM images are demonstrated on the Fig. 4. The particles of PA450 sample have an arbitrary shape and consist of disordered graphene sheets (Fig. 4a, b). Conversion of the TEM images to binary color (black and white) scheme allows us to emphasize details of the graphene layers morphology on sub-nanoscale (insert in Fig. 5a, d). In

Fig. 2 CO₂ adsorption isotherms (a) and CO₂ uptake (b) at 25 °C

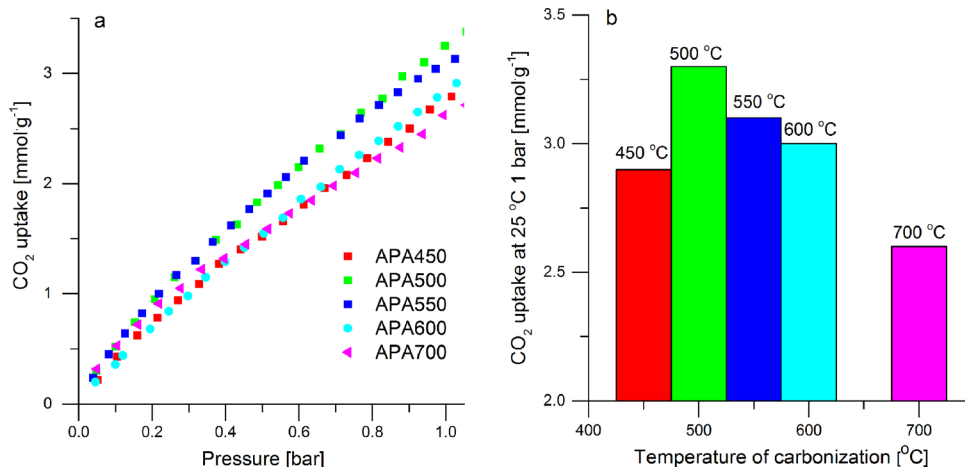
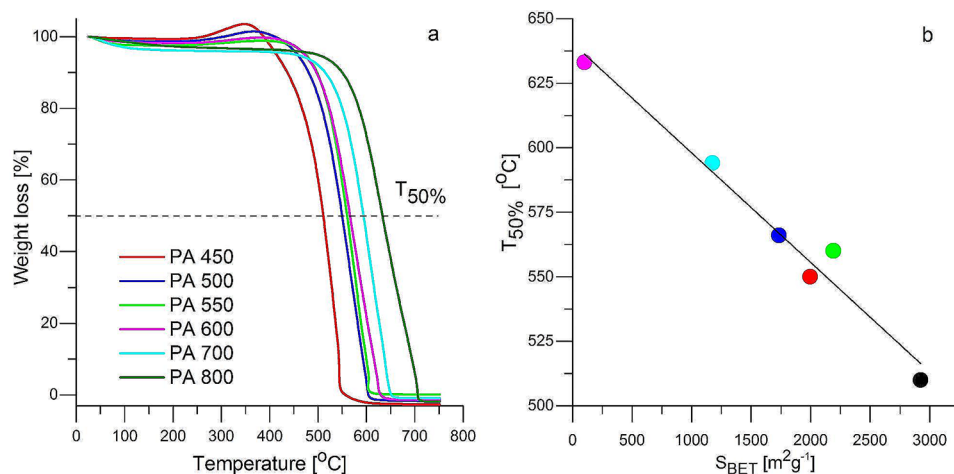


Fig. 3 (a) TG-curves of the carbonized asphalts. (b) BET surface area of activated asphalt-derived porous carbons versus temperature of 50% conversion of the carbonized asphalts



the PA450 sample randomly arranged graphene nanolayers are short (0.5–2 nm) and strongly curved. The interlayer distance is in the range of 0.4–1.3 nm with the distribution maximum of 0.71 nm. These distances were calculated from the analysis of the radial intensity profiles obtained after FFT analysis of the images (Fig. 5g).

TEM images of the PA600 sample demonstrates a more ordered structure compared to the PA450 carbon. The distance between graphene layers is 0.4–0.7 nm with the distribution maximum of 0.49 nm that is considerably smaller than the corresponding values of the PA450 sample. However, the length of the single graphene layer is longer (close to 3 nm) and the anisotropy of the structure becomes clearer (Figs. 4c and d and 5b and e).

The texture of the PA800 sample is evident (Fig. 4 e, f). The graphene layers in this sample are relatively extended and ordered. The length of graphene layers is 0.5–5 nm and distance between them is 0.4–0.6 nm with the distribution maximum of 0.44 nm (Figs. 4e and f and 5c, f and h). Thus, the petroleum asphalt carbonized at 450 °C has the most defective and disorder structure. This is probably why the PA450 carbon precursor is more labile to the oxidation. These structural defects formed during asphalt carbonization are suggested to expand and collapsed to larger pores at thermal treatment with lower energy barriers. Moreover, the small size of crystallites and their disordered arrangement leads to a high specific surface area of carbon materials after the activation [27]. This is confirmed for the APA450 sample.

The carbonization at 500–600 °C produces the relatively stable carbon precursors. Its stable structure further provides a mild activation of the material. Therefore, the pre-carbonization procedure of petroleum asphalts at 500–600 °C promotes the formation of carbon materials with microporous structure. The carbonization of the asphalt at 800 °C leads to the sharp reduction of the structural defects and decrease of the interlayer space. The latter significantly

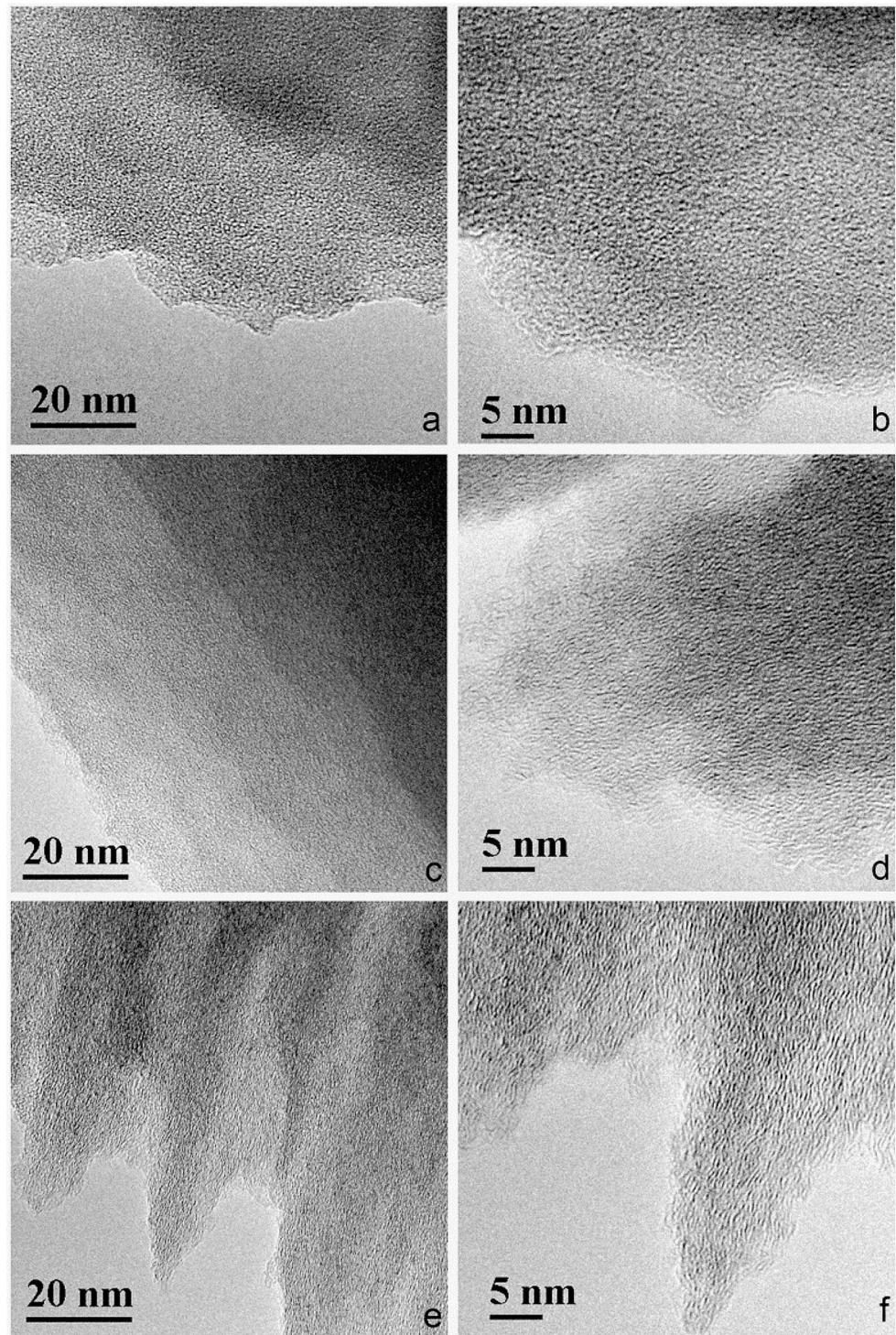
hampers the oxidation process and, therefore, the formation and expansion of pores during the activation of the porous carbon precursors.

The surface functional groups of the carbonized petroleum asphalts were identified using the FTIR spectroscopy. The obtained FTIR spectra are shown in Fig. 6. After carbonization at 450 °C there are absorption bands at 2820–2950 cm⁻¹ and 1350–1450 cm⁻¹ on the spectra. These bands are assigned to stretching vibrations of C–H bond in CH₃– and –CH₂– groups, respectively [28]. In addition, the FTIR spectra exhibit absorption bands at 3000–3050 and 700–900 cm⁻¹, which are usually attributed to vibrations of C–H bonds in aromatic rings. The absorption bands at 1500–1600 cm⁻¹ correspond to C=C bond vibrations representing the aromatic rings [29, 30]. The FTIR spectra have wide absorption band at 3250–3500 cm⁻¹ which corresponds to stretching vibrations of O–H bonds in hydroxyl functional groups.

After carbonization of the asphalt at 600 °C the intensities of the FTIR absorption bands at 2820–2950 cm⁻¹ and 1350–1450 cm⁻¹ decrease. When the carbonization temperature is 600–700 °C, the intensity of absorption bands at 3000–3050 cm⁻¹ and 700–900 cm⁻¹ also reduces. A new absorption band appears at 1200–1300 cm⁻¹ in the FTIR spectra of the asphalt samples carbonized at the temperatures of 700–800 °C. These bands correspond to stretching vibrations of C–O bonds in phenolic ethers and lactones [31]. Thus, the increase of carbonization temperature up to 700 and 800 °C induces the condensation reactions of alcohols, phenols and aromatic structures. The disappearance of the above-mentioned IR bands at the carbonization temperatures above 600 °C indicates the thermal destruction of the surface functional groups. Thus, the surface of the carbonized samples is “cleaned” and its reactivity decreases.

The C–O, C–O–C, C–O–H and some alkyl surface groups are known to affect the chemical activation process and promote an extension of the porosity of carbon materials.

Fig. 4 TEM images of the carbonized asphalt samples: PA450 (a, b), PA600 (c, d) and PA800 (e, f)

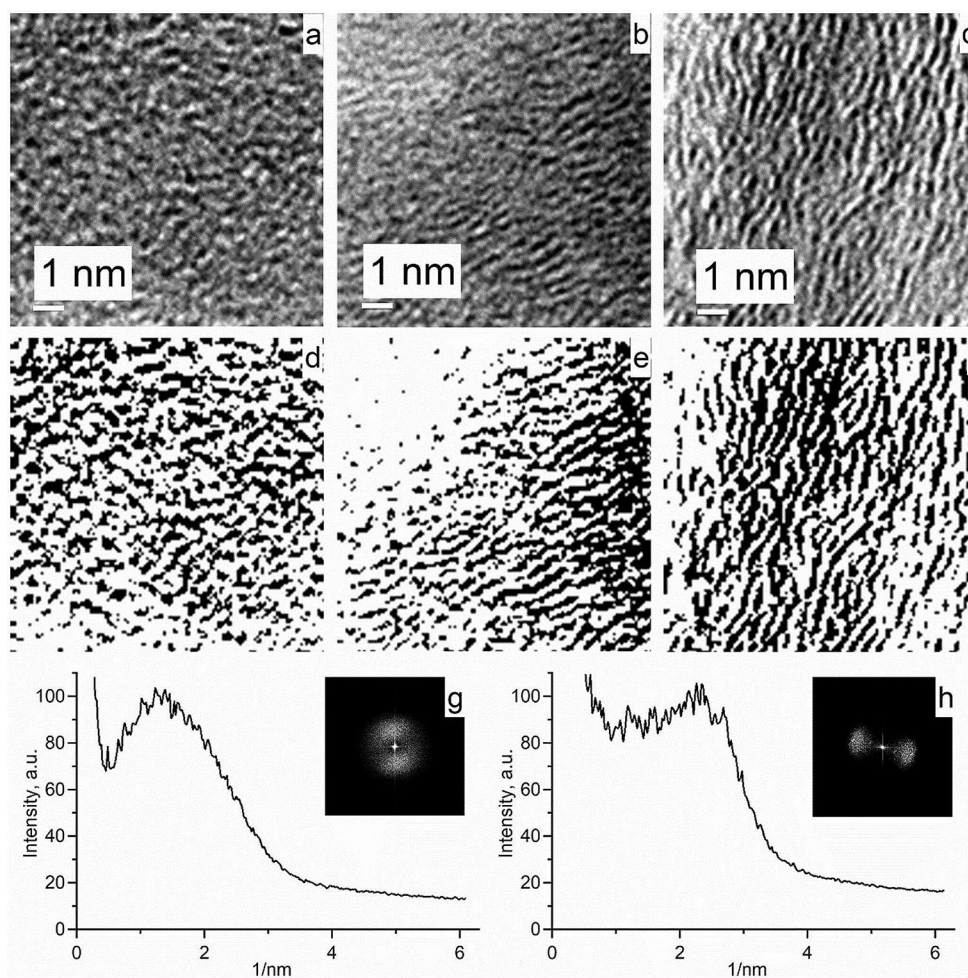


Firstly, these functional groups react with KOH to form C–O–K intermediate species that act as active sites. The obtained particles further react with the carbon precursors. This process directs the formation of porous structure of the ACs samples [32, 33]. Thus, the textural properties of activated carbon materials such as BET surface area and pore

size distribution can be controlled by optimizing the conditions of the pre-carbonization process.

Figure 7 shows the Raman spectra of the carbonized asphalts after fluorescence correction. In the Raman spectra there are peaks: one is near 1345 cm^{-1} assigned to a disordered graphitic lattice vibration mode with A_{1g} symmetry (D peak), and another is near 1595 cm^{-1} attributed to a

Fig. 5 TEM images and binary images following filtering and threshold selection of the asphalt carbonized samples: PA450 (a, d), PA600 (b, e) и PA800 (c, f). Graphs of the profile of the radial intensity of the contrast obtained after FFT of the images which shown in the insets: sample PA450 (g), sample PA800 (h)



graphitic lattice vibration mode with E_{2g} symmetry (G peak) [34]. In addition, low intensity peaks appear in the spectrum at 1447 and 1160 cm^{-1} . It indicates the presence of various defects in the graphite-like structures of the sample [34, 35]. The observed peak at 1251 cm^{-1} corresponds to diamond-like structures [36]. As it is seen in Fig. 7, the position of the bands recorded in the Raman spectra does not change significantly at the same time as the intensity of the peaks decreases by ~ 4 times when the carbonization temperature increases from 450 to $600\text{ }^\circ\text{C}$. Further increase of the asphalt carbonization temperature leads to completely disappearing bands at 1447 and 1160 cm^{-1} , corresponding to various defects of disordered graphite-like structures. In this way, the structure is ordered. The results of Raman spectroscopy are consistent with TEM and IR spectroscopy data.

It can be concluded that the carbonization temperature of petroleum asphalt affect the structural defects, distance between the graphene layers, the reactivity and thermal stability of the carbon precursor. These specificities contribute in varying degrees to formation the porous structure of the activated carbon. Thus, we have proposed the simple and

effective way to control the porous structure of the porosity of activated carbons derived from petroleum asphalt.

4 Conclusion

In this work we consider how carbonization temperature of petroleum asphalt affects the further chemical activation process and porous structure of the activated carbons (ACs). It is found that the carbonization temperature mainly influences the structural defects and the graphene interlayer space in carbonized asphalts. It has a direct effect on the porous structure formed during the further chemical activation of the carbonized asphalts. The reactivity of the carbon precursor affects the formation of oxidation active sites on the surface of carbonized asphalts.

The specific surface area of the ACs is shown to be predicted from the temperature of 50% mass loss of the carbonized petroleum asphalt. The carbonization of petroleum asphalt at 500 – $600\text{ }^\circ\text{C}$ makes it possible to obtain a relatively stable carbon precursor providing mild activation. At such conditions the microporous carbon materials are produced.

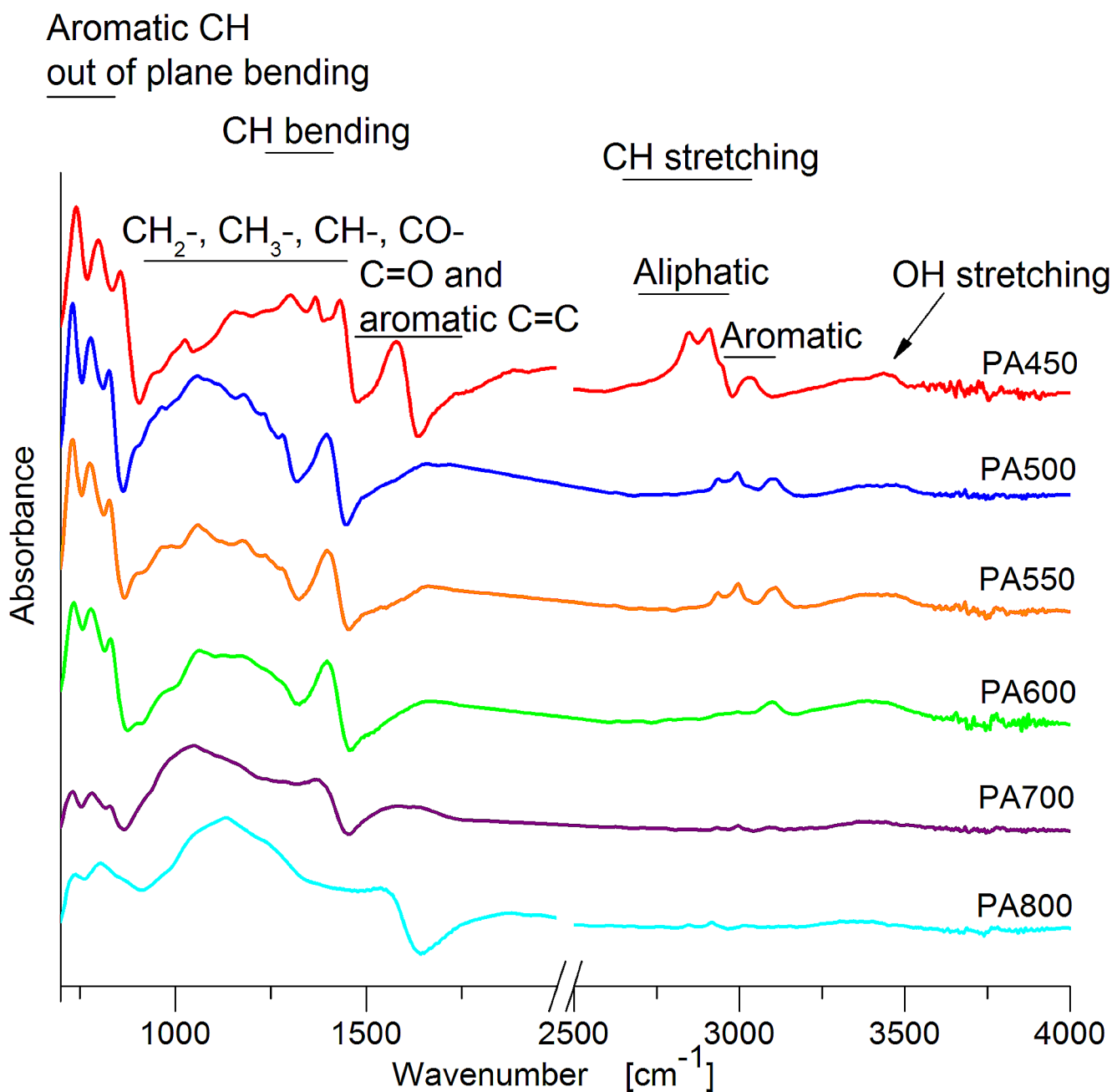


Fig. 6 FTIR spectra of the carbonized petroleum asphalt

The carbonization of the asphalt at higher temperatures (800 °C) decreases the structural inhomogeneity and the graphene interlayer space. Such ACs are more stable to the oxidation reactions occurring on the activation stage. The carbonization temperature of 500–600 °C is revealed to be optimal for the further activation of the carbonized petroleum asphalts. The KOH activation of the petroleum asphalts carbonized at 500–600 °C provides microporous carbon with the high specific surface area (about 2000 m²g⁻¹) and the CO₂ uptake (3.3 mmolg⁻¹).

Thus, it is relatively easy to obtain a carbon adsorbent with a high specific surface area and a CO₂ capacity from inexpensive and non-recyclable petroleum asphalt by careful tuning of the carbonization temperature. We believe that such carbon adsorbents will find wider applications beyond CO₂ capture. This is the subject of our further research and developments.

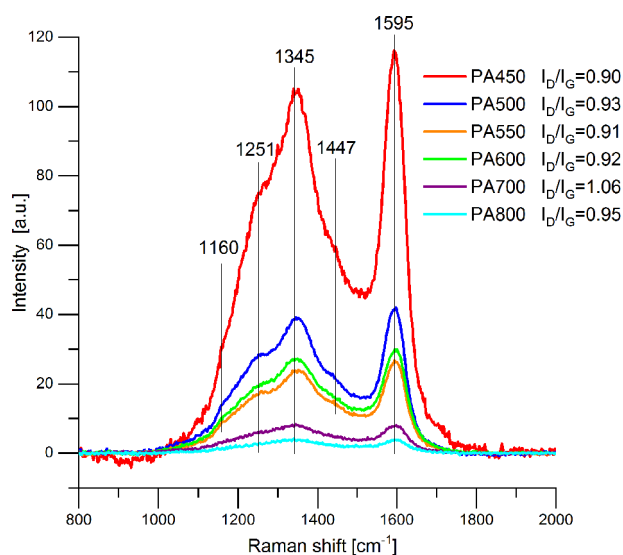


Fig. 7 Raman spectra carbonized petroleum asphalt

Acknowledgements The studies were carried out using facilities of the shared research center “National Center of Investigation of Catalysts” at Boreskov Institute of Catalysis and shared research center at the Omsk Scientific Center, Siberian Branch of the Russian Academy of Sciences.

Author contributions O.V. Gorbunova took part in methodology, writing & editing the article, investigation. O.N. Baklanova contributed in writing and editing of the article. T.I. Gulyaeva, A.V. Vasilevich, A.B. Arbuzov, M.V. Trenikhin carried out measurements and investigation. A.V. Lavrenov took part in supervision.

Funding This work was supported by the Ministry of Science and Higher Education of the Russian Federation within the governmental order for Boreskov Institute of Catalysis (FWUR-2024-0039).

Data availability Not Applicable.

Declarations

Ethical approval Not Applicable.

Competing interests There are no competing interests to declare.

References

- Marsh, H., Reinoso, F.R.: Activated Carbon Elsevier (2006)
- Yang, L., Feng, Y., Cao, M., Yao, J.: Two-step preparation of hierarchical porous carbon from KOH-activated wood sawdust for supercapacitor. *Mater. Chem. Phys.* **238**, 121956–121973 (2019). <https://doi.org/10.1016/j.matchemphys.2019.121956>
- Lia, C., Wang, Y., Xiao, N., Li, H., Ji, Y., Guo, Z., Liu, C., Qiu, J.: Nitrogen-doped porous carbon from coal for high efficiency CO₂ electrocatalytic reduction. *Carbon*. **151**, 46–52 (2019). <https://doi.org/10.1016/j.carbon.2019.05.042>
- Zhang, S., Shi, X., Wróbel, R., Chen, X., Mijowska, E.: Low-cost nitrogen-doped activated carbon prepared by polyethyl- enimine (PEI) with a convenient method for supercapacitor

- application. *Electrochim. Acta*. **294**, 183–191 (2019). <https://doi.org/10.1016/j.electacta.2018.10.111>
- Zbair, M., Ainassaari, K., Drif, A., Ojala, S., Bottlinger, M., Pirilä, M., Brahmi, R.: Toward new benchmark adsorbents: Preparation and characterization of activated carbon from argan nut shell for bisphenol A removal. *ESPR*. **25**, 1869–1882 (2017). <https://doi.org/10.1007/s11356-017-0634-6>
- Siddiqui, M.N., Ali, I., Asim, M., Chanbasha, B.: Quick removal of nickel metal ions in water using asphalt-based porous carbon. *J. Mol. Liq.* **308**, 113078–113087 (2020). <https://doi.org/10.1016/j.molliq.2020.113078>
- Jang, E., Choi, S.W., Lee, K.B.: Effect of carbonization temperature on the physical properties and CO₂ adsorption behavior of petroleum coke-derived porous carbon. *Fuel*. **248**, 85–92 (2019). <https://doi.org/10.1016/j.fuel.2019.03.051>
- Liu, J., Liu, Y., Li, P., Wang, L., Zhang, H., Liu, H., Liu, J., Wang, Y., Tian, W., Wang, X., Li, Z., Wu, M.: Fe-N-doped porous carbon from petroleum asphalt for highly efficient oxygen reduction reaction. *Carbon*. **126**, 1–8 (2018). <https://doi.org/10.1016/j.carbon.2017.10.004>
- Strausz, O.P., Peng, P., Murgich, J.: About the colloidal nature of asphaltenes and the mw of covalent monomeric units. *Energy Fuels*. **1**, 809–822 (2002). <https://doi.org/10.1021/ef0002795>
- Groenzin, H., Mullins, O.C., Eser, S., Mathews, J., Yang, M.G., Jones, D.: Molecular size of asphaltene solubility fractions. *Energy Fuels*. **17**, 498–503 (2003). <https://doi.org/10.1021/ef010239g>
- Javed, H., Luong, D.X., Lee, C.-G., Zhang, D., Tour, J.M., Alvarez, P.J.J.: Efficient removal of bisphenol-A by ultra-high surface area porous activated carbon derived from asphalt. *Carbon*. **140**, 441–448 (2018). <https://doi.org/10.1016/j.carbon.2018.08.038>
- Liang, W., Zhang, Y., Wang, X., Wu, Y., Zhou, X.: Asphalt-derived high surface area activated porous carbons for the effective adsorption separation of ethane and ethylene. *Chem. Eng. Sci.* **162**, 192–202 (2017). <https://doi.org/10.1016/j.ces.2017.01.003>
- Heidarinejad, Z., Dehghani, M.H., Heidari, M., Javedan, G., Ali, I., Sillanpää, M.: Methods for preparation and activation of activated carbon: A review. *Environ. Chem. Lett.* **18**, 393–415 (2020). <https://doi.org/10.1007/s10311-019-00955-0>
- Yamashita, Y., Ouchi, K.: Influence of alkali on the carbonization process-I: Carbonization of 3,5-dimethylphenol-formaldehyde resin with NaOH. *Carbon*. **20**, 41–45 (1982). [https://doi.org/10.1016/0008-6223\(82\)90072-0](https://doi.org/10.1016/0008-6223(82)90072-0)
- Katesa, J., Junpiromand, S., Tangsathitkulchai, C.: Effect of carbonization temperature on properties of char and activated carbon from coconut shell. *Suranaree J. Sci. Technol.* **20**, 269–278 (2013). <https://www.thaiscience.info/journals/Article/SJST/10966578.pdf>
- Sun, S., Yu, Q., Li, M., Zhao, H., Wang, Y., Ji, X.: Effect of carbonization temperature on characterization and water vapor adsorption of coffee-shell activated carbon. *Adsorpt. Sci. Technol.* **38**, 9–10 (2020). <https://doi.org/10.1177/0263617420950994>
- Zhai, D., Li, B., Du, H., Wang, G., Kang, F.: The effect of pre-carbonization of mesophase pitch-based activated carbons on their electrochemical performance for electric double-layer capacitors. *J. Solid State Electrochem.* **15**, 787–794 (2011). <https://doi.org/10.1007/s10008-010-1156-z>
- Gorbunova, O.V., Baklanova, O.N., Gulyaeva, T.I., Arbuzov, A.B., Trenikhin, M.V., Lavrenov, A.V.: Effect of thermal pretreatment on porous structure of asphalt-based carbon. *J. Mater. Sci.* **57**, 7239–7249 (2022). <https://doi.org/10.1007/s10853-022-07106-x>
- Jagiello, J., Olivier, J.P.: 2D-NLDFT adsorption models for carbon slit-shaped pores with surface energetical heterogeneity and geometrical corrugation. *Carbon*. **55**, 70–80 (2013). <https://doi.org/10.1016/j.carbon.2012.12.011>

20. Zhu, W., Miser, D.E., Chan, W.G., Hajaligol, M.R.: HRTEM investigation of some commercially available furnace carbon blacks. *Carbon*. **42**, 1841–1845 (2004). <https://doi.org/10.1016/j.carbon.2004.01.077>
21. Kruk, M., Jaroniec, M., Ryoo, R., Joo, S.H.: Characterization of ordered mesoporous carbons synthesized using mem-48 silicas as templates. *Phys. Chem. B*. **104**, 796–7968 (2000). <https://doi.org/10.1021/jp000861u>
22. Gorbunova, O.V., Baklanova, O.N., Gulyaeva, T.I.: Porous structure of PEG-mediated silica controlled by solution pH. *Microporous Mesoporous Mater*. **307**, 110468–110472 (2020). <https://doi.org/10.1016/j.micromeso.2020.110468>
23. Thommes, M., Kaneko, K., Neimark, A.V., Olivier, J.P., Rodriguez-Reinoso, F., Rouquerol, J., Sing, K.S.W.: Physisorption of gases, with special reference to the evaluation of surface area and pore size distribution (IUPAC Technical Report). *Pure Appl. Chem*. **87**, 1051–1069 (2015). <https://doi.org/10.1515/pac-2014-1117>
24. Seaton, N.A., Walton, J.P.R.B., Quirke, N.: A new analysis method for the determination of the pore size distribution of porous carbons from nitrogen adsorption measurements. *Carbon*. **27**, 13–22n (1989). [https://doi.org/10.1016/0008-6223\(89\)90035-3](https://doi.org/10.1016/0008-6223(89)90035-3)
25. Abd, A.A., Naji, S.Z., Hashim, A.S., Othman, M.R.: Carbon dioxide removal through physical adsorption using carbonaceous and non-carbonaceous adsorbents: A review. *J. Environ. Chem. Eng*. **8**, 104142–104164 (2020). <https://doi.org/10.1016/j.jece.2020.104142>
26. Thermal Analysis Application No HB 451, Mettler Toledo TA Application Handbook Elastomers: Vol.2. https://www.mt.com/us/en/home/supportive_content/matchar_apps/MatChar_HB451, accessed 22.03.24
27. Kaneko, K., Ishii, C., Ruike, M., Kuwabara, H.: Origin of super-high surface area and microcrystalline graphitic structures of activated carbons. *Carbon*. **30**, 1075–1088 (1992). [https://doi.org/10.1016/0008-6223\(92\)90139-N](https://doi.org/10.1016/0008-6223(92)90139-N)
28. Ding, H., Hesp, S.A.M.: Variable-temperature Fourier-transform infrared spectroscopy study of asphalt binders from the SHRP materials reference. *Fuel*. **298**, 120819 (2021). <https://doi.org/10.1016/j.fuel.2021.120819>
29. Xing, C., Liu, L., Cui, Y., Ding, D.: Analysis of base bitumen chemical composition and aging behaviors via atomic force microscopy-based infrared spectroscopy. *Fuel*. **264**, 116845 (2020). <https://doi.org/10.1016/j.fuel.2019.116845>
30. Hou, X., Lv, S., Chen, Z., Xiao, F.: Applications of Fourier transform infrared spectroscopy technologies on asphalt materials. *Measurement*. **121**, 304–316 (2018). <https://doi.org/10.1016/j.measurement.2018.03.001>
31. Burg, P., Cagniant, D.: Characterization of Carbon Surface Chemistry. *Chem. Phys. Carbon*. **30**, 129–175 (2008). <https://doi.org/10.1201/9781420042993.ch3>
32. Ehrburger, P., Addoun, A., Addoun, F., Ddonnet, J.B.: Carbonization of coals in the presence of alkaline hydroxides and carbonates: Formation of activated carbons. *Fuel*. **65**, 1447–1449 (1986). [https://doi.org/10.1016/0016-2361\(86\)90121-3](https://doi.org/10.1016/0016-2361(86)90121-3)
33. Chunlan, L., Shaoping, X., Yixiong, G., Shuqin, L., Changhou, L.: Effect of pre-carbonization of petroleum cokes on chemical activation process with KOH. *Carbon*. **43**, 2295–2301 (2005). <https://doi.org/10.1016/j.carbon.2005.04.009>
34. Sadezky, A., Muckenhuber, H., Grothe, H., Niessner, R., Pöschl, U.: Raman microspectroscopy of soot and related carbonaceous materials: Spectral analysis and structural information. *Carbon*. **43**, 1731–1742 (2005). <https://doi.org/10.1016/j.carbon.2005.02.018>
35. Moseenkov, S.I., Kuznetsov, V.L., Zolotarev, N.A., Kolesov, B.A., Prosvirin, I.P., Ishchenko, A.V., Zavorin, A.V.: Investigation of Amorphous Carbon in Nanostructured Carbon materials (a comparative study by TEM, XPS, Raman Spectroscopy and XRD). *Materials*. **16**, 1112 (2023). <https://doi.org/10.3390/ma16031112>
36. Chuang, C.-C., Liu, W.-L., Chen, W.-J., Huang, J.-H.: Temperature and substrate dependence of structure and growth mechanism of carbon nanofiber. *Appl. Surf. Sci*. **254**, 4681–4687 (2008). <https://doi.org/10.1016/j.apsusc.2008.01.097>

Publisher's Note Springer Nature remains neutral with regard to jurisdictional claims in published maps and institutional affiliations.

Springer Nature or its licensor (e.g. a society or other partner) holds exclusive rights to this article under a publishing agreement with the author(s) or other rightsholder(s); author self-archiving of the accepted manuscript version of this article is solely governed by the terms of such publishing agreement and applicable law.